

## One-Dimensional Mechanistic Model for Flow Boiling Pressure Drop in Small- to Micro- Passages

Dereje SHIFERAW<sup>1</sup>, Mohamed MAHMOUD<sup>2</sup>, Tassos G. KARAYIANNIS<sup>2,\*</sup>, David B.R. KENNING<sup>2</sup>

\* Corresponding author: Tel.: ++44 (0)1895 267132; Fax: ++44 (0)1895 256392; Email: tassos.karayiannis@brunel.ac.uk

1: Cal Gavin Process Intensification Ltd, Station Road, Warwickshire, B49 5ET, UK

2: School of Engineering and Design, Brunel University

**Abstract** Accurate predictions of two-phase pressure drop in small to micro diameter passages are necessary for the design of compact and ultra-compact heat exchangers which find wide application in process and refrigeration industries and in cooling of electronics. A semi-mechanistic model of boiling two-phase pressure drop in the confined bubble regime is formulated, following the three-zone approach of Thome et al. (2004) for heat transfer. The total pressure drop is calculated by time-averaging the respective pressure drop values of single-phase liquid, elongated bubble with a thin liquid film and single-phase vapour. The model results were compared with experimental data collected for a wide range of diameter tubes (4.26, 2.88, 2.02, 1.1 and 0.52 mm) for R134a at 6 – 12 bar.

**Keywords:** Two phase, Pressure Drop, Flow Boiling, Small diameter tube

### 1. Introduction

Miniaturization of power and refrigeration systems requires the transfer of high heat fluxes at low temperature differences (high heat transfer coefficients) to achieve efficient use of energy. However, although it is generally recognized that heat transfer coefficients can be higher for flow boiling in mini- and micro-channels than in conventional channels the reduction in cross-section is limited by the increase in pressure drop and the pumping power required to drive the flow. Therefore, accurate prediction of pressure drop is critical for design and optimization of these devices. Many studies confirmed that the two phase total pressure drop in small and micro tubes is higher and increases with decreasing internal tube diameter, Tong et al. (1997), Huo et al. (2007), Revellin and Thome (2007). Tong et al. (1997) hypothesized that this could be due to the fact that the boundary layer becomes thinner as the tube diameter decreases resulting in a higher velocity gradient that in turn produces larger pressure drop.

Widely used classical models are based on homogenous flow, separated flow, and annular two phase flow models. These have been extended to microchannel flow boiling by modifying coefficients to fit experimental data. Most often, they failed to take account of the new features of boiling phenomena in small and micro scale thermal systems. On the other hand, there is very limited number of theoretical models that are based on the flow regimes predominantly observed in small to micro passages. It is now highly desirable to develop mechanistic models for flow boiling in small to micro-channels that are well validated by experiments. Also, the fact that pressure drop could depend on the local flow structure suggest the need for simplified mechanistic models that are based on flow regimes.

A number of studies have reported that there is a clear effect of decreasing tube diameter on flow pattern and their transition boundaries, (Damianides and Westwater (1988), Coleman and Garimella (1999), Zhao and Bi (2001), Chen et al. (2006), Kawahara et al. (2002) and Revellin and Thome (2007)).

These include but are not limited to the absence of stratified flow in horizontal channels, diminishing of churn flow and the appearance of additional flow patterns that are not common in normal tubes. These have been mainly attributed to the predominance of surface tension force over gravity. Chen et al. (2006) studied the effect of tube diameter on flow pattern transition boundaries for the tubes of 4.26-1.1 mm diameter using R134a and showed that the slug/churn and churn/annular transition lines shift towards higher quality as the tube diameter decreased. They also indicated that the slug (periodic) flow regime can exist up to a quality range as high as 0.5 especially at low mass flux values. These deviations from the conventional understanding raise doubt in the applicability of design methods based on empirical correlations of boiling data in large channels and suggest the necessity for new flow regime based predicting methods. Garimella (2004) developed a flow regime based model for pressure drop during condensation of refrigerants inside round, square and rectangular passages of hydraulic diameter in the range of 1- 5 mm. Validation of their model results against experimentally measured value indicated that flow regime based models yield significantly better pressure drop predictions than traditionally used empirical correlations, which are primarily based on air-water mixture flow in large diameter tubes. Unlike flow boiling in large tubes, mechanistic modeling of heat transfer and pressure drop can be promising in small-to micro- diameter tubes for a number of reasons. For instance, as stated above, most flow visualization studies reported the absence or diminishing of dispersed bubble and churn flows, and better defined liquid/film interface as the tube diameter decreases. In addition, flow regimes in small diameter tubes (4.26 -1.1 mm) at low vapour quality ( $x < 0.3 - 0.5$ ) are dominated by slug flow regime with mostly no trails of small bubbles at the bubble tail. At high quality, annular flow regime is expected. However, beyond a quality of about 0.4 - 0.5 dryout is deduced in many studies from the heat transfer measurements. Therefore, a model based on

periodic flow bubble slugs is likely to represent the prevailing condition and can be a reasonable approach to predict heat transfer and pressure drop. Hence, a one-dimensional pressure drop model for slug flow regime is presented here. The model employs a similar approach to the three-zone evaporation model developed by Thome et al. (2004) for predicting flow boiling heat transfer. The results are compared with experimental data collected using R134a for five stainless steel tubes of internal diameter 4.26, 2.08, 2.01, 1.1 and 0.52 mm. Other parameters were varied in the range: mass flux 100 – 500 kg/m<sup>2</sup>s; pressure 6 – 12 bar; quality up to 0.9; heat flux 13 - 150 kW/m<sup>2</sup>.

## 2. Thome 3-zone heat transfer model

### 2.1 Assumptions

The assumptions in Thome et al. (2004) model are

1. Confined-bubble flow, sequence: liquid, vapour + evaporating film, vapour only.
2. Fluctuation period  $t_b$  set by nucleation period at a single upstream site.

This period is not determined by experimental observation but by modifying a correlation based on pool boiling to optimising the fit of the complete heat transfer model to a large data base for heat transfer coefficients for a range of fluids and conditions:

$$t_b = \left( \frac{3328}{q} \right)^{1.74} \left( \frac{P_{crit}}{p} \right)^{0.87} \quad (1)$$

The dimensional nature of this correlation indicates that further development of the model is required.

3. Negligible film thickness  $\delta$  compared to channel cross-section dimensions,  $\delta \ll D$ .
4. Negligible transport of liquid by motion of the film (from 3).
5. Negligible effect on flow area for vapour (from 3).
6. Homogeneous flow. A liquid slug and the head of the bubble immediately behind it have the same velocity, the “pair velocity”  $U_p$ , given by

$$U_p = G \left[ \frac{x}{\rho_v} + \frac{1-x}{\rho_l} \right] \quad (2)$$

and the residence times of alternating liquid  $t_l$  and vapour (with and without liquid film)  $t_v$  during a cycle of period  $t_b$  are given by

$$\frac{t_l}{t_b} = \frac{1}{1 + \frac{\rho_l x}{\rho_v (1-x)}}, \quad \frac{t_v}{t_b} = \frac{1}{1 + \frac{\rho_v (1-x)}{\rho_l x}} \quad (3)$$

where  $x(z)$  is the local time-averaged mass fraction of vapour at axial distance  $z$ .

7. Thermal equilibrium between phases, so that  $x$  may be calculated from a time-averaged enthalpy balance for a specified heat input per length of channel with all phases at the local saturation temperature.

8. The initial liquid film thickness of formation  $\delta_0(z)$  was calculated from an empirical correlation  $\delta_0/D = F(Bo)$  given by Moriyama and Inoue (1996) which was corrected by a factor equal 0.29 by Dupont et al. (2004) as:

$$\frac{\delta_0}{D} = 0.29 \left( \frac{V_l}{U_p D} \right)^{0.28} \left[ \left( 0.07 Bo^{0.41} \right)^{-8} + 0.1^{-8} \right]^{-1/8} \quad (4)$$

where the Bond number is defined by

$$Bo = \rho_l D U_p^2 / \sigma \quad (5)$$

This is the only feature of the model that involves surface tension  $\sigma$ , which is generally assumed to be the dominant influence on the progression from small to mini- to micro-channels.

9. After formation, the film is assumed to be stationary relative to the wall. Its thickness  $\delta(t)$  decreases by evaporation and therefore depends on the model for heat transfer. The Thome et al. (2004) model assumes constant, uniform heat flux  $q$  from the wall to whatever fluid is in contact with it (liquid, liquid film, vapour). For liquid and vapour, the bulk temperature is assumed to be  $T_{sat}(p)$ , where  $p$

is the time-averaged pressure, and heat transfer coefficients are obtained from conventional correlations for fully-developed flow with  $U_p(z)$  as the bulk velocity, despite the possibly short lengths of slugs and bubbles and consequent internal circulation patterns. The assumptions for the film are steady conduction with the liquid-vapour interface at  $T_{sat}(p)$ . The film thickness at time  $t$  after formation is then

$$\delta = \delta_0 - qt / \rho_l h_{lv} \quad (6)$$

The film is assumed to break up at a minimum thickness  $\delta_{min}$ , the value being chosen to optimise the fit of the entire heat transfer model to a database. A more physically based choice may be of the order of the wall roughness, see Thome et al. (2004). The evaporation time  $t_e$  is given by

$$t_e = (\delta_0 - \delta_{min}) \rho_l h_{lv} / q \quad (7)$$

If  $t_e < t_v$ , there is a period of vapour-only flow equal to  $t_e - t_v$ .

If  $t_e > t_v$ , the film evaporates to a thickness at the end of the bubble given by

$$\delta_{end} = \delta_0 - qt_v / \rho_l h_{lv} \quad (8)$$

It is assumed that survival of the film has no influence on conditions in the following liquid slug.

The equations for change in film thickness would be modified if a different heat transfer model were used, e.g. transient conduction in a film on a wall of finite thickness.

## 2.2 Comments on heat transfer model

The assumption of homogeneous time-averaged flow is central to the Thome et al. (2004) heat transfer model, leading to a relatively straightforward approach to predicting time-averaged wall temperature for a constant wall heat flux without the need to track the development of individual bubbles. Consequently local fluctuations in pressure or velocity are not modelled. Only the time-averaged homogeneous velocity  $U_p(z)$  can be

used for the bulk phase velocities and inputs to the local mechanistic models such as liquid film thickness.

During the time fractions corresponding to single phase liquid or vapour flow, the heat transfer coefficients  $\alpha_l, \alpha_v$  are calculated from correlations for fully developed flow using  $U_p(z)$  and the relevant single phase properties. In film flow, the heat transfer coefficient is estimated for conduction through the mean film thickness  $\delta_m$ :

$$\alpha_f = 2k_l / (\delta_0 + \delta_{\min})$$

or

$$\alpha_f = 2k_l / (\delta_0 + \delta_{\text{end}}) \quad (9)$$

Time-averaging wall temperature with constant wall heat flux is equivalent to calculating the time-averaged heat transfer coefficient  $\alpha(z)$  from

$$\frac{1}{\alpha} = \frac{1}{\alpha_l} \frac{t_l}{t_b} + \frac{1}{\alpha_f} \frac{t_e}{t_b} + \frac{1}{\alpha_v} \frac{(t_v - t_e)}{t_b} \quad (10)$$

This mechanistic method replaces in the homogeneous model the calculation of  $\alpha$  from a single-phase convective correlation of the form  $Nu = f(Re, Pr)$ , using expressions for homogeneous properties such as

$$c_h = xc_v + (1-x)c_l \quad (11)$$

$$\frac{1}{k_h} = \frac{x}{k_v} + \frac{(1-x)}{k_l} \quad (12)$$

$$\frac{1}{\rho_h} = \frac{x}{\rho_v} + \frac{(1-x)}{\rho_l} \quad (13)$$

$$(a) \quad \frac{1}{\mu_h} = \frac{x}{\mu_v} + \frac{(1-x)}{\mu_l} \quad \text{or}$$

$$(b) \quad \mu_h = x\mu_v = (1-x)\mu_l \quad (14)$$

For liquid and vapour slugs of finite length, the homogeneous flow assumption is an approximation and the assumption of local

thermal equilibrium between phases leads to inconsistencies. There can be no superheating of the liquid or vapour so the enthalpy of the thin film must be negligible and all the heat transferred to the liquid and vapour phases in the absence of a thin film must somehow be transferred by internal mixing to a liquid-vapour interface to cause evaporation.

### 3. Pressure drop model

Applying this approach to the prediction of pressure drop, a direct consequence of the homogeneous flow and local thermal equilibrium assumptions is that the time averaged gravitational and acceleration contributions to the pressure gradient may be calculated from the axial distribution of heat input and Eq.(13). For uniform heat flux, vertical upward flow in a circular tube

$$x = \frac{4q}{Gh_{lv}} \frac{z}{D},$$

$$\frac{dp_{grav}}{dz} = -\rho_h g = -\frac{\rho_l g}{\left(1 + \frac{4qv_{lv}}{DGh_{lv}v_l} z\right)},$$

$$\frac{dp_{acc}}{dz} = -G \frac{dU_p}{dz} = -\frac{4Gqv_{lv}}{Dh_{lv}} \quad (15)$$

The time-averaged wall shear stress and frictional pressure gradient are calculated by time-sharing between estimates for the liquid-only, vapour + liquid film and vapour-only regimes:

$$\tau_w = \tau_l \frac{t_l}{t_b} + \tau_f \frac{t_e}{t_b} + \tau_v \frac{(t_v - t_e)}{t_b},$$

$$\frac{dp_{fric}}{dz} = -\frac{4\tau_w}{D} \quad (16)$$

The total time-averaged pressure gradient is the sum of the three time-averaged contributions:

$$\frac{dp}{dz} = \frac{dp_{grav}}{dz} + \frac{dp_{acc}}{dz} + \frac{dp_{fric}}{dz} \quad (17)$$

For the single-phase regimes, the Thome et al. (2004) approach of using correlations for heat transfer in fully-developed flow based on the local homogeneous velocity  $U_p$  is applied to the estimation of the friction coefficients, with the same reservations noted in Section 2. In the examples used later in this paper, the Reynolds number calculated from the homogeneous velocity and the single phase properties is always greater than 2000, so a standard correlation such as Blasius equation for fully-developed turbulent flow is used:

$$\tau_w = \frac{0.0791}{\text{Re}^{1/4}} \frac{\rho U_p^2}{2}, \quad \text{Re} = \frac{DU_p \rho}{\mu} \quad (18)$$

where  $\rho$ ,  $\mu$  are for liquid-only or vapour-only.

The presence of a thin evaporating liquid film during interval  $t_e$  may have three hydrodynamic consequences.

(i) The flow area for the vapour flow is reduced. In the simple approach presented here, this effect is neglected, consistent with assumptions 3 and 4 in the Thome model above that  $\delta \ll D$ . (There may be circumstances in which this condition is not valid, which should be checked with Eq.(4)). The bulk velocity in the vapour is then equal to the velocity of the vapour without a film, assumed to be  $U_p$ .

(ii) Instabilities at the liquid-vapour interface may increase its effective roughness, an effect that is known to be important in large channels. For now, it is assumed that the interface remains smooth.

(iii) Motion of the liquid film with an interfacial velocity of  $U_i$  reduces the velocity for calculation of the interfacial shear stress  $\tau_i$  exerted by the vapour to  $(U_p - u_i)$ . Eq.(18) becomes

$$\tau_i = \frac{0.0791}{\text{Re}^{1/4}} \frac{\rho_v (U_p - u_i)^2}{2},$$

$$\text{Re} = \frac{D(U_p - u_i) \rho_v}{\mu_v} \quad (19)$$

This effect is estimated by an approximate model that does not follow the nonlinear reduction in film thickness with time. Instead, quasi-steady, parallel flow is assumed in a film

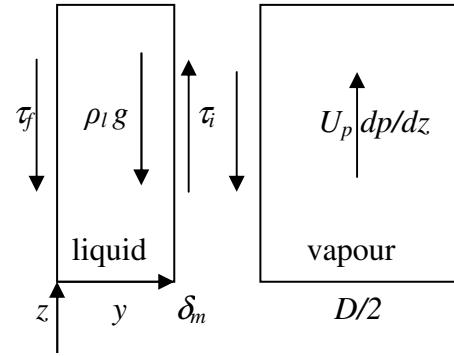


Fig.1. Thin film model

of constant and uniform thickness  $\delta_m$  equal to the average of the initial thickness  $\delta_0$  and the final thickness  $\delta_{min}$  or  $\delta_{end}$ , as calculated by the methods in the heat transfer model.

In a vertical tube, the film is subjected to the same total pressure gradient  $dp/dz$  as the adjacent gas phase, a gravitational body force  $\rho_l g$ , a wall shear stress  $\tau_f$  and an interfacial shear stress  $\tau_i$ , Fig. 1. Consistent with the steady-flow approximation, the changes in momentum of the film are assumed negligible. For a planar approximation consistent with  $\delta_m \ll 1$ , the velocity distribution for laminar flow in the film is given by

$$u = \frac{\tau_i}{\mu_l} y + \left[ \frac{dp}{dz} + \rho_l g \right] \frac{y}{\mu_l} \left( \frac{y}{2} - \delta_m \right) \quad (20)$$

$$u_i = \frac{\tau_i}{\mu_l} \delta_m - \left[ \frac{dp}{dz} + \rho_l g \right] \frac{\delta_m^2}{2\mu_l} \quad (21)$$

$$\text{and} \quad \tau_f = \tau_i - \left[ \frac{dp}{dz} + \rho_l g \right] \delta_m \quad (22)$$

The pressure gradient in the vapour during the thin-film period is not equal to the time-averaged pressure gradient and is given by

$$\begin{aligned} \frac{dp}{dz} &= \frac{dp_{grav}}{dz} + \frac{dp_{acc}}{dz} + \frac{dp_{fric}}{dz} \\ &= -\rho_v \left[ g + U_p \frac{dU_p}{dz} \right] - \frac{4\tau_i}{D \left( 1 - 2 \frac{\delta_m}{D} \right)} \quad (23) \\ &\approx -\rho_v \left[ g + U_p \frac{dU_p}{dz} \right] - \frac{4\tau_i}{D} \end{aligned}$$

The wall shear stress  $\tau_f(z)$  is obtained by simultaneous solution of Eq. (19), (21-23) with inputs  $U_p(z)$ ,  $dU_p/dz(z)$  and  $\delta_a$ . The time-averaged wall shear stress and frictional pressure gradient are calculated from Eq.(16). This semi-mechanistic estimate replaces the fully homogeneous flow calculation by substituting equivalent fluid properties into Eq. (18). As noted above, the time-averaged gravitational and acceleration components of the pressure gradient are calculated from the homogeneous flow model.

#### 4. Range of validity of model

A mechanistic model for confined-bubble flow should not be applied to any other flow regime but the model does not define its own limits. The assumption of phase equilibrium implies that the single nucleation site coincides with  $x = 0$  and that a bubble of negligible length instantly fills the channel. The wall superheat required for nucleation and the motion of bubbles before confinement are not considered.

The assumption that the transport of liquid in the film is negligible implies that the liquid plug between confined bubbles remains until  $x = 1$ . The mean velocity in the film is given by

$$\bar{u} = \frac{\tau_i}{2\mu_l} \delta_m - \left[ \frac{dp}{dz} + \rho_l g \right] \frac{\delta_m^2}{3\mu_l} \quad (24)$$

A sufficient condition for the disappearance of the liquid slug is

$$\rho_l \bar{u} \delta_m \frac{t_e}{t_b} = \frac{DG(1-x)}{4} \quad (25)$$

but the regime of confined bubbles with

smooth laminar films may well break down at smaller values of  $x$  due to wave formation on the films or instability of the liquid plug between bubbles.

### 5. Comparison with data for $\Delta p$

#### 5.1 Experimental conditions

Pressure differences across small channels are usually measured from plenum to plenum, so they include inlet and entry losses. Pressure measurements are rarely made at intermediate stations. Wen and Kenning (2004) found that the greatest variability in pressure drop occurred in the section in which boiling was initiated. The data for R134a used in this paper were obtained in thin-walled tubes directly heated by alternating current, with pressure tappings and bulk temperature thermocouples incorporated in the inlet and outlet electrodes. These were joined to adiabatic sections with internal diameter exactly matching the test section, so that there were no pressure losses associated with inlet and outlet plena. A correction was calculated for fully-developed liquid flow over the short distance from the inlet pressure tapping to the calculated point  $x = 0$ , since the actual point of first nucleation could not be observed. Inlet subcooling was small. No correction was applied for the very short length of adiabatic two-phase flow in the outlet electrode. The exit flow patterns were recorded by high-speed video in the transparent adiabatic section. The estimates of experimental error in the measured pressure drop are  $\pm 0.34\%$ . The details of the experimental facility can be found in Chen et al. (2006).

#### 5.3 Comparisons of homogeneous flow and 3-zone models with data

As stated above the model is based on the assumption that slug flow regime is the dominant flow pattern and considering smooth vapour-liquid interface. The flow pattern studies of Chen (2006) indicated that the prevailing flow regime in small tubes is slug flow up to a quality as high as 0.5. In addition, Chen (2006) also pointed out that the so called “small tube characteristics”, i.e. confined flow,

slimmer vapour slug, thinner liquid film and smoother vapour-liquid interface, were observed when the tube diameter was reduced to 2.01 mm and further to 1.10 mm for the working fluid R134a at pressures of 6 – 12 bar. Therefore, the model is recommended for such flow conditions, i.e. slug flow with smooth vapour-liquid interface. Hence, below an example is presented for the pressure drop results of 2.01 and 1.1 mm tubes. Figure 2 shows the experimental total two phase pressure drop as a function of exit quality, which for a fixed length depends on the applied heat flux, compared to the current 3-zone and homogeneous pressure drop models at 8 bar pressure and mass flux values of 300 and 400 kg/m<sup>2</sup>s, for the 2.01 and 1.1 mm tubes. It is clear from this figure that, the difference between the 3-zone and homogeneous flow models is negligible. This is because the 3-zone model was developed based on the assumption of homogeneous flow and because, for these conditions, the liquid film is too thin to greatly affect the pressure drop across a bubble. Generally, the figure also shows that the two pressure drop models have correctly predicted the trend of the pressure drop with exit quality up to  $x_e = 0.6$ .

The mean absolute error between the measured and predicted values, for the two cases presented in Fig. 2, was found to be in the order of 13 % except at  $G = 300 \text{ kg/m}^2 \text{ s}$  and  $D = 2.01 \text{ mm}$  where it was in the order of 20 %. In the current calculations,  $0.3 \mu\text{m}$  was used as a value for the end film thickness ( $\delta_{end}$ ) as proposed by Dupont et al. (2004) in the heat transfer 3-zone model.

Figure 3 depicts the global comparison of the present experimental data and the 3-zone pressure drop model. As seen in Figs. 3 (a) and (b), the data for the relatively larger tubes (4.26 and 2.88 mm) are predicted fairly well almost within  $\pm 35\%$ . The slight scattering observed in these tubes could be related to the fact that in these tubes churn flow was observed, which has a different liquid/film interface than the model assumption.

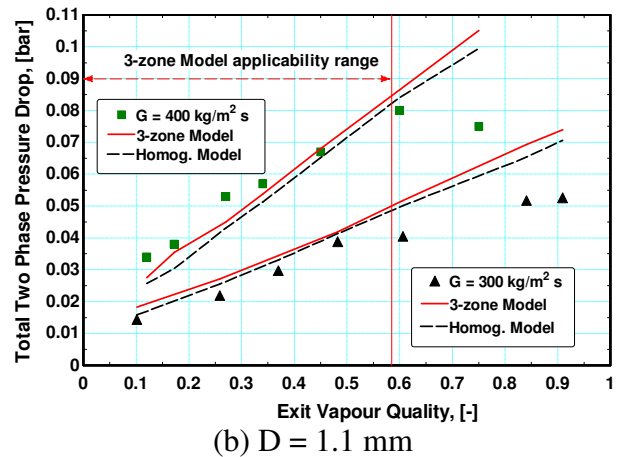
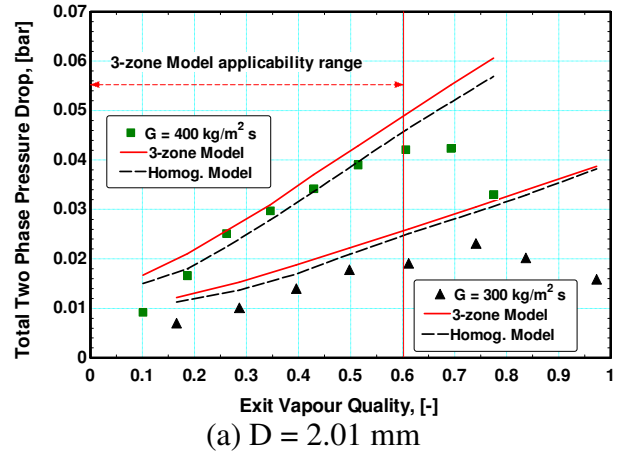
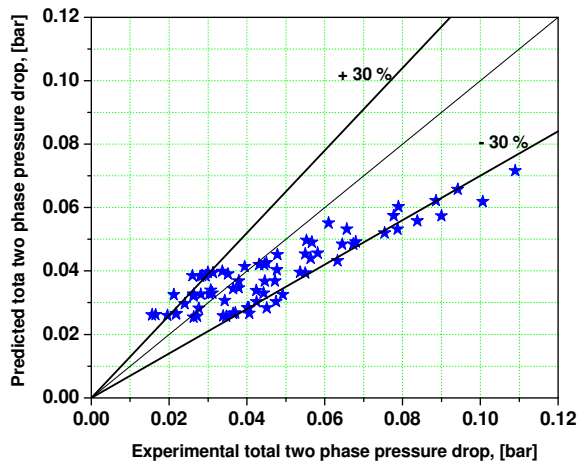


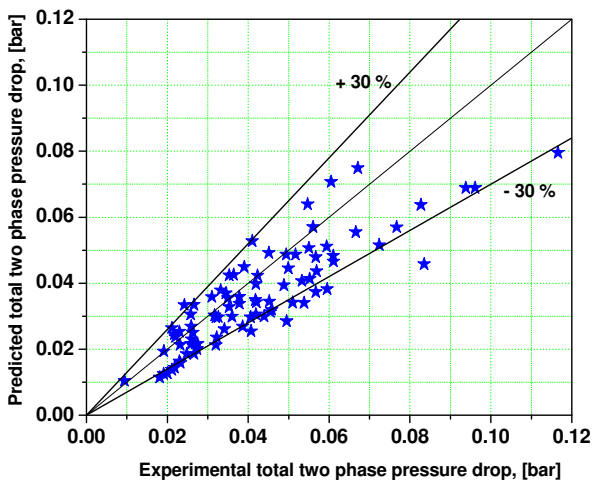
Figure 2 Total pressure drop as a function of exit quality as predicted by 3-zone and homogeneous pressure drop models at 8 bar.

For the 2.01 and 1.1 mm tubes in Figures 3 (c) and (d) respectively, the prediction becomes relatively better than the 4.26 and 2.88 mm tubes. This could be due to the relatively frequent appearance of slug flow with a nearly smooth film interface, which is the basis of the model. In Fig. 3 (e), the smallest tube (0.52 mm) results are also reasonably predicted, particularly in the very small pressure drop region. This region represents the very small exit quality below which the flow pattern is elongated bubble with short lengths which corresponds roughly with the assumption of the model. Beyond this quality, the bubble becomes very long with a pattern which has the characteristics of annular flow. This explains the tendency of the model to under-predict the experimental values in the high pressure drop region, i.e. high exit quality.

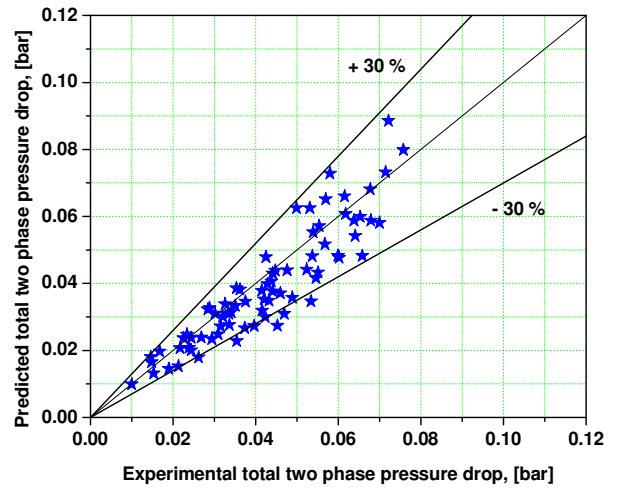
Generally, the 3-zone pressure drop model works reasonably well for cases, where slug flow with relatively smooth interface is expected. However, it requires further work, particularly in finding a better assumption for film thickness and also incorporating film waviness. Overall, the preliminary one-dimensional model has predicted the pressure drop data with a Mean Absolute Error (MAE) of 23, 20, 16.8, 16.3 and 22 % for the 4.26, 2.88, 2.01, 1.1 and 0.52 mm tubes respectively. The percentages of the data within  $\pm 30\%$  are 71.8, 76.5, 89.8, 87.7 and 67.2 % respectively.



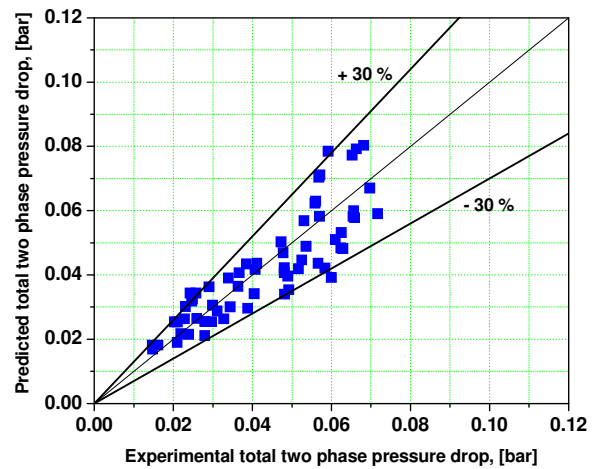
(a)



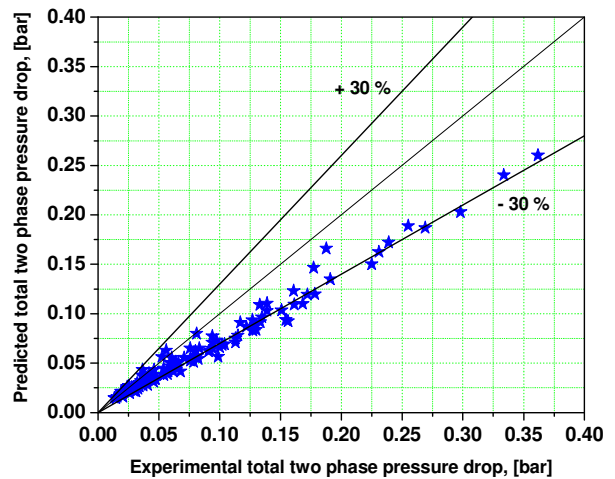
(b)



(c)



(d)



(e)

Figure 3 Comparison of current pressure drop model with data for the different tube diameters: (a) 4.26 mm, (b) 2.88 mm, (c) 2.01 mm, (d) 1.1 mm and (e) 0.52 mm.

## 6. Conclusions

A new three-zone pressure drop model for slug flow regime with an assumption of smooth liquid film interface was developed. The model development followed a similar approach as the three-zone heat transfer model of Thome et al. (2004). During confined bubble flow, the pressure gradient was obtained using a three zone model that included parallel flow of a liquid film and a vapour core up to the dryout point in each bubble. The model has the capability of predicting the pressure drop data for R134a at 8 bar with Mean Absolute Error (MAE) of 23, 20, 16.8, 16.3 and 22 % for the 4.26, 2.88, 2.01, 1.1 and 0.52 mm tubes respectively. However, there are features that require further study. These include a better theoretical model for predicting the initial film thickness during slug flow, considering additional effect of coalescence and film waviness on heat transfer and determination of the model's validity range so that it can include annular flow regime once the liquid slug vanishes. For example, in the smallest tube (0.52 mm), the dominant flow pattern was annular flow with unstable film interface. The model is developed with an assumption of smooth film interface, a condition which can be achieved only at very low quality range. To extend the model's applicability by predicting transition to annular flow, it will be necessary to consider the transport of liquid by thick films. Also, the effect of film instability should be considered. These improvements to the pressure drop model would also apply to the heat transfer model.

## NOMENCLATURE

$Bo$	Bond number, see Eq. 5
$C$	Any property
$D$	internal diameter, m
$f$	pair frequency (Hz); friction Coef.
$g$	gravitational acceleration, $m/s^2$
$G$	mass flux, $kg/m^2 s$
$h_{lv}$	latent heat of vaporization, $J/kg$
$k$	Thermal conductivity, $W/m K$
$L$	length, $m$
$\dot{m}$	mass flow rate, $kg/s$

$Nu$	Nusselt number
$P$	pressure, bar
$Pr$	Prandtl number
$q$	heat flux, $W/m^2$
$t$	time, sec
$t_b$	pair period, sec
$T$	Temperature, K
$R$	Radius, $m$
$Re$	Reynolds number, see Eqs. 18, 19
$U$	velocity, $m/sec$
$x$	vapour quality
$y$	transverse distance
$z$	axial distance
<b>Greek</b>	
$\alpha$	Heat transfer coefficient, $W/m^2 K$
$\delta$	liquid film thickness, $m$
$\Delta$	change
$\mu$	dynamic viscosity, $kg/m s$
$\nu$	kinematic viscosity, $m^2/s$
$\rho$	density, $kg/m^3$
$\sigma$	surface tension, $N/m$
$\tau$	shear stress ( $N/m^2$ )
<b>Subscripts</b>	
$acc$	Acceleration
$CB$	confined bubble
$crit$	critical
$df$	drift flux
$dry$	dryout zone
$dry film$	dryout of liquid film
$e$	evaporation
$end$	end of the liquid film
$film$	liquid film between bubble and wall
$fric$	Frictional
$g$	gas
$go$	gas only
$grav$	Gravitational
$h$	homogeneous
$i$	interface
$l$	liquid
$lf$	liquid film
$lo$	liquid only
$ls$	liquid slug
$m$	mean
$min$	minimum
$opt$	optimum
$p$	pair
$ref$	reference
$sat$	saturation

<i>tot</i>	total
<i>tp</i>	two phase
<i>v</i>	vapour
<i>vs</i>	vapour slug
<i>O</i>	initial
<i>w</i>	Wall

## REFERENCES

- L. Chen, Y.S. Tian, and T.G. Karayiannis. The effect of tube diameter on vertical two-phase flow regimes in small tubes. *International Journal Heat Mass Transfer*, 49: 4220-4230, 2006.
- M.G. Cooper. Saturated nucleate pool boiling – a simple correlation. In *first UK National Heat Transfer Conference, IChemE Symposium*, Series 86, 2:785-793, 1984.
- J.W. Coleman and S. Garimella. Characterization of two-phase flow patterns in small diameter round and rectangular tubes. *International Journal of Heat and Mass Transfer*, 42:2869-2881, 1999.
- C.A. Damianides and J.W. Westwater. Two-phase flow patterns in a compact heat exchanger and in small tubes. In *Second UK National Conference on Heat Transfer*, 11:1257-1268, 1988.
- V. Dupont, J.R. Thome, A.M. Jacobi, Heat transfer model for evaporation in microchannels, Part II: comparison with the database, *International Journal Heat Mass Transfer*, 47:3387-3401, 2004.
- Garimella S. Condensation flow mechanisms in micro-channels: Basis for pressure drop and heat transfer models. *Heat Transfer Engineering* 25(3):104 – 116, 2004.
- X. Huo, Y. S. Tian, and T. G. Karayiannis. R134a flow boiling heat transfer in small diameter tubes. *Advances in Compact Heat Exchangers*, R. T. Edwards, Inc., 5:95 -111, 2007.
- A. Kawahara, P.M-Y. Chung, and M. Kawaji. Investigation of two-phase flow patterns, void fraction and pressure drop in a micro-channel. *International Journal Multiphase Flow*, 28(9):1411–1435, 2002.
- M. Kureta, T. Kobayashi, K. Mishima, and H. Nishihara. Pressure drop and heat transfer for flow boiling of water in small diameter tubes, *JSME International Journal, Series B*, 41(4):871-879, 1998.
- K. Mishima and T. Hibiki. Some characteristics of air-water two-phase flow in small diameter vertical tubes. *International Journal Multiphase Flow*, 22(4):703 – 712, 1996.
- K. Moriyama, A. Inoue. Thickness of the liquid film formed by a growing bubble in a narrow gap between two horizontal plates. *Journal Heat Transfer*, 118:132-139, 1996.
- R. Revellin and J.R. Thome. Adiabatic two-phase frictional pressure drops in microchannels. *Experimental Thermal Fluid Science*, 31(7):673-685, 2007.
- J.R. Thome, V. Dupont, and A.M. Jacobi. Heat transfer model for evaporation in microchannels, Part I: presentation of the model. *International Journal Heat Mass Transfer*, 47:3375-3385, 2004.
- W. Tong, A.E. Bergles, and M.K. Jensen. Pressure drop with highly subcooled flow boiling in small-diameter tubes, *Experimental Thermal and Fluid Science*, 15:202–212, 1997.
- T.S. Zhao and Q.C. Bi. Co-current air-water two-phase flow patterns in vertical triangular microchannels, *International Journal of Multiphase Flow*, 27:765-782, 2001.
- D.S. Wen and D.B.R. Kenning. Two phase pressure drop of water during flow boiling in a vertical narrow channel. *Experimental thermal and Fluid science* 28 (2-3):131 – 138, 2004.